

Daily Precipitation Statistics for South America: An Intercomparison between NCEP Reanalyses and Observations

VIVIANE B. S. SILVA, VERNON E. KOUSKY, AND R. WAYNE HIGGINS

NOAA/NWS/NCEP/Climate Prediction Center, Camp Springs, Maryland

(Manuscript received 7 April 2010, in final form 7 October 2010)

ABSTRACT

In this study, the authors document the extent to which the precipitation statistics of the new CFS reanalysis (CFSR) represent an improvement over the earlier reanalyses: the NCEP–NCAR reanalysis (R1) and the NCEP–DOE Second Atmospheric Model Intercomparison Project (AMIP-II) reanalysis (R2). An intercomparison between the CFSR, R1, R2, and observations over South America was made for the period 1979–2006. The CFSR shows notable improvements in the large-scale precipitation patterns compared with the previous reanalyses (R1 and R2). In spite of these improvements, the CFSR has substantial biases in intensity and frequency of occurrence of rainfall events. Over west-central Brazil, the core region of the South American monsoon system (SAMS), the CFSR displays a dry bias during the onset phase of the SAMS wet season and a wet bias during the peak and decay phases of the SAMS wet season. The CFSR also displays a dry bias along the South American coast near the mouth of the Amazon and along the east coast of northeastern Brazil. A wet bias exists in all seasons over southeast Brazil and over the Andes Mountains.

1. Introduction

The National Centers for Environmental Prediction–National Center for Atmospheric Research (NCEP–NCAR) reanalysis (R1; Kalnay et al. 1996) was developed in the early 1990s with the objective of reanalyzing historical data using a state-of-the-art model and data assimilation system. Even though R1 is one of the most popular and widely used climate datasets currently in existence, there are nevertheless a number of documented problems with it (e.g., Kanamitsu et al. 2002). To address some of these problems, Kanamitsu et al. (2002) produced the NCEP–Department of Energy (DOE) Second Atmospheric Model Intercomparison Project (AMIP-II) reanalysis (R2) for the period 1979–2002. The R2 used an improved data assimilation system and forecast model that featured upgraded physics and soil moisture forcing. Both R1 and R2 were extended forward in real time using climate data assimilation systems (CDAS1 and CDAS2, respectively).

Since the mid-1990s the NOAA/Climate Prediction Center (CPC) has used the NCEP–NCAR reanalysis products and their real-time extension forward in time in operational climate monitoring and prediction activities. The NCEP has recently developed a new generation of reanalysis products (Saha et al. 2010) as part of the Climate Forecast System Reanalysis and Reforecast (CFSRR) project. This project is driven by NCEP's intraseasonal-to-interannual prediction needs. In comparison with the earlier NCEP reanalyses (R1 and R2), there are three major differences in the Climate Forecast System Reanalysis (CFSR): 1) higher horizontal and vertical resolution (an atmosphere at horizontal resolution of spectral T382, ~35 km, and vertical resolution of 64 sigma-pressure hybrid levels), 2) the guess forecast is generated from a coupled atmosphere–ocean–sea ice–land system, and 3) historical satellite radiance measurements are assimilated.

The CFSR will replace R1 as the reference dataset for real-time monitoring at the CPC. Before replacing R1 and R2 it is important to document the extent to which CFSR represents an improvement over the earlier reanalyses. The objectives of this study are to document the CFSR precipitation biases over South America and to provide diagnostics that can lead to future CFS model improvements. Precipitation was chosen to be the focus

Corresponding author address: Viviane B. S. Silva, NOAA/Climate Prediction Center, 5200 Auth Rd., Room 811, Camp Springs, MD 20746.
E-mail: Viviane.Silva@noaa.gov

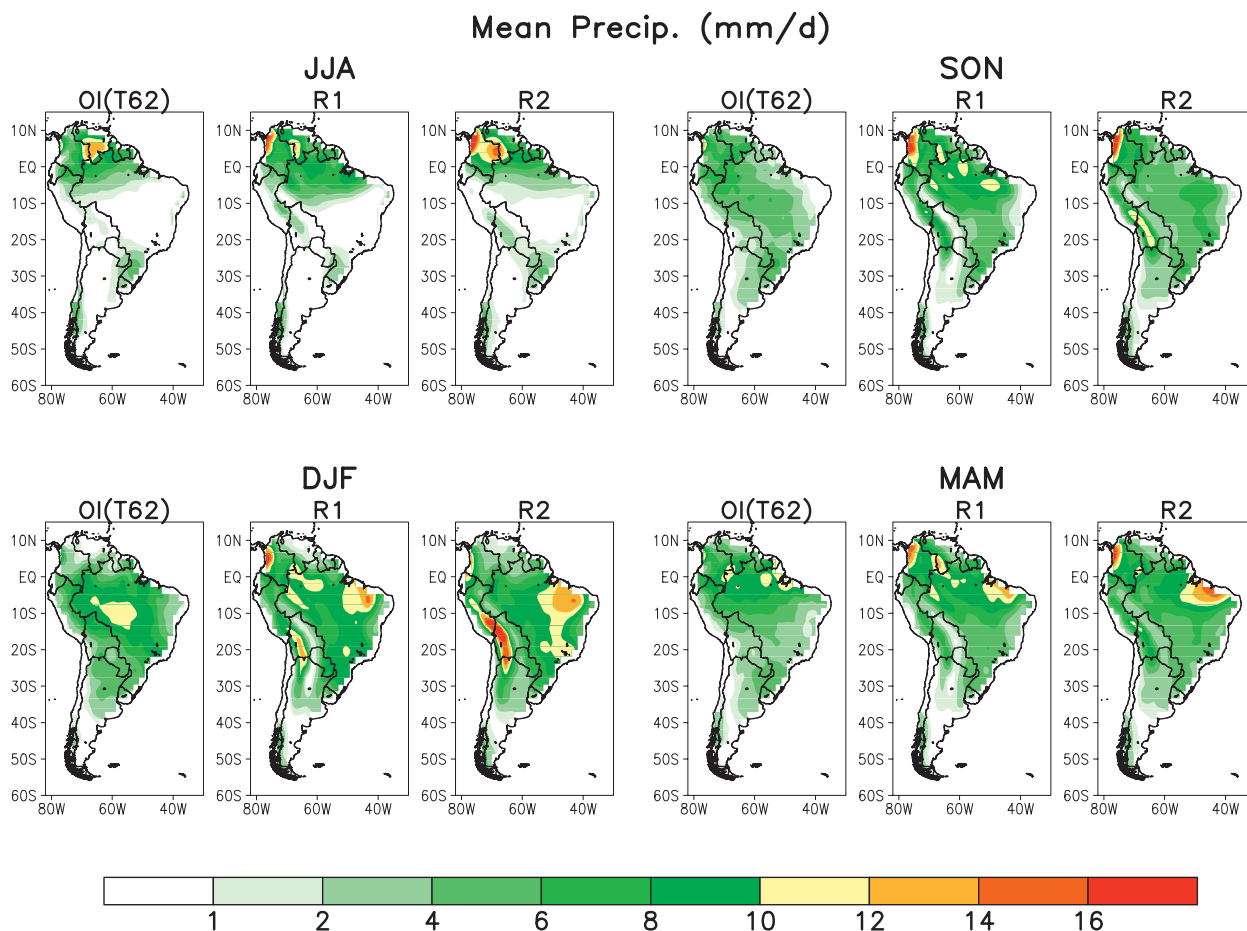


FIG. 1. Mean daily precipitation (mm day^{-1}) for OI(T62), R1, and R2. Results are shown by season and are based on daily data for the period 1979–2006.

of this study because it is a critical variable in model prediction and because it is not assimilated into the CFS data assimilation system (i.e., precipitation is an independent measure of model performance).

2. Data and methods

In the mid-1990s the CPC began a comprehensive project to improve the analysis of gauge-based daily precipitation over the Americas. The goal of this project is to develop improved historical and real-time daily, monthly, and seasonal gauge-only precipitation analyses to support climate prediction, monitoring, and assessment activities, as well as to serve as a research dataset for studies on weather and climate variability. The approach has been incremental, by first focusing on the United States and then by expanding this effort to include the remainder of North, Central, and South America (Higgins et al. 2000; Silva et al. 2007). Recently, the analysis technique has been improved and the domain

expanded to cover the global land areas (Chen et al. 2008).

The CPC global gridded precipitation analysis (Chen et al. 2008) is used in this study as the basis for intercomparisons with the new CFSR model-based precipitation analyses over South America. The observed precipitation analyses are prepared using Global Telecommunications System (GTS) daily reports and additional reports provided by many hydrographic and agricultural agencies in countries around the globe. The analyses are based on the optimal interpolation (OI) method of Gandin (1965). The gauge-based analysis was created originally on a 0.125° latitude–longitude grid over global land areas and integrated to a 0.5° latitude–longitude grid for release to the general public. In this study, the gauge analysis at its raw resolution is averaged to T62 and T382 grids for quantitative comparisons with the reanalyses (R1, R2, and CFSR). While the daily ending time of the gauge reports varies from country to country, the day-1 gauge analysis is valid for

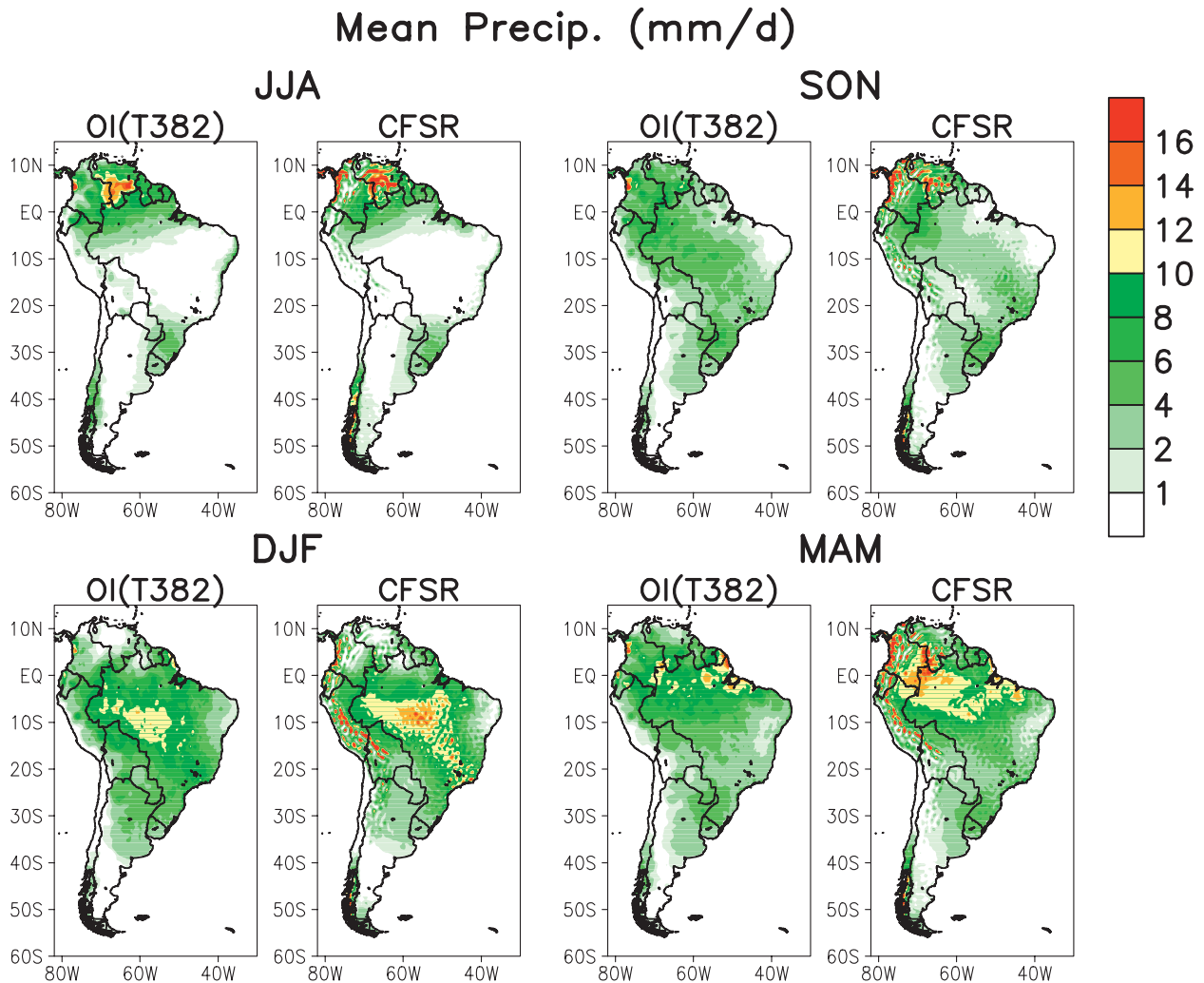


FIG. 2. Mean daily precipitation (mm day^{-1}) for OI(T382) and CFSR. Results are shown by season and are based on daily data for the period 1979–2006.

the window from 1200 UTC on day 0 to 1200 UTC on day 1 over all of South America.

To compare the reanalysis precipitation fields to observations the OI analyses were regridded to two resolutions: 1) the same resolution as the CFSR (~ 35 km) and 2) the same resolution as R1 and R2 (~ 187 km). In each case the reanalysis daily rainfall totals were computed for the same 24-h period as the OI analysis. Hereafter, we will refer to the low-resolution OI analysis as OI(T62) and the high-resolution OI analysis as OI(T382). In this study we will focus on the following statistics for 1979–2006: 1) the mean daily precipitation, 2) the ratio of variance [$R1/OI(T62)$, $R2/OI(T62)$, $CFSR/OI(T382)$], 3) the temporal correlation [$R1$ vs $OI(T62)$, $R2$ vs $OI(T62)$, and $CFSR$ vs $OI(T382)$], and 4) the probability ratio [$CFSR/OI(T382)$] of daily precipitation exceeding selected threshold amounts. Our emphasis is on seasonal

patterns [June–July–August (JJA), September–October–November (SON), December–January–February (DJF), and March–April–May (MAM)] and seasonal differences (biases).

3. Results

a. Mean daily precipitation

The South American mean daily rainfall (1979–2006) patterns for OI(T62), R1, and R2 during the four seasons JJA, SON, DJF, and MAM are shown in Fig. 1. During JJA, the patterns in R1 and R2 are similar to OI(T62), with the largest rainfall maximum over northern South America and a weaker maximum over southern Brazil. There are substantial differences in the patterns in SON, with both R1 and R2 having maxima over the

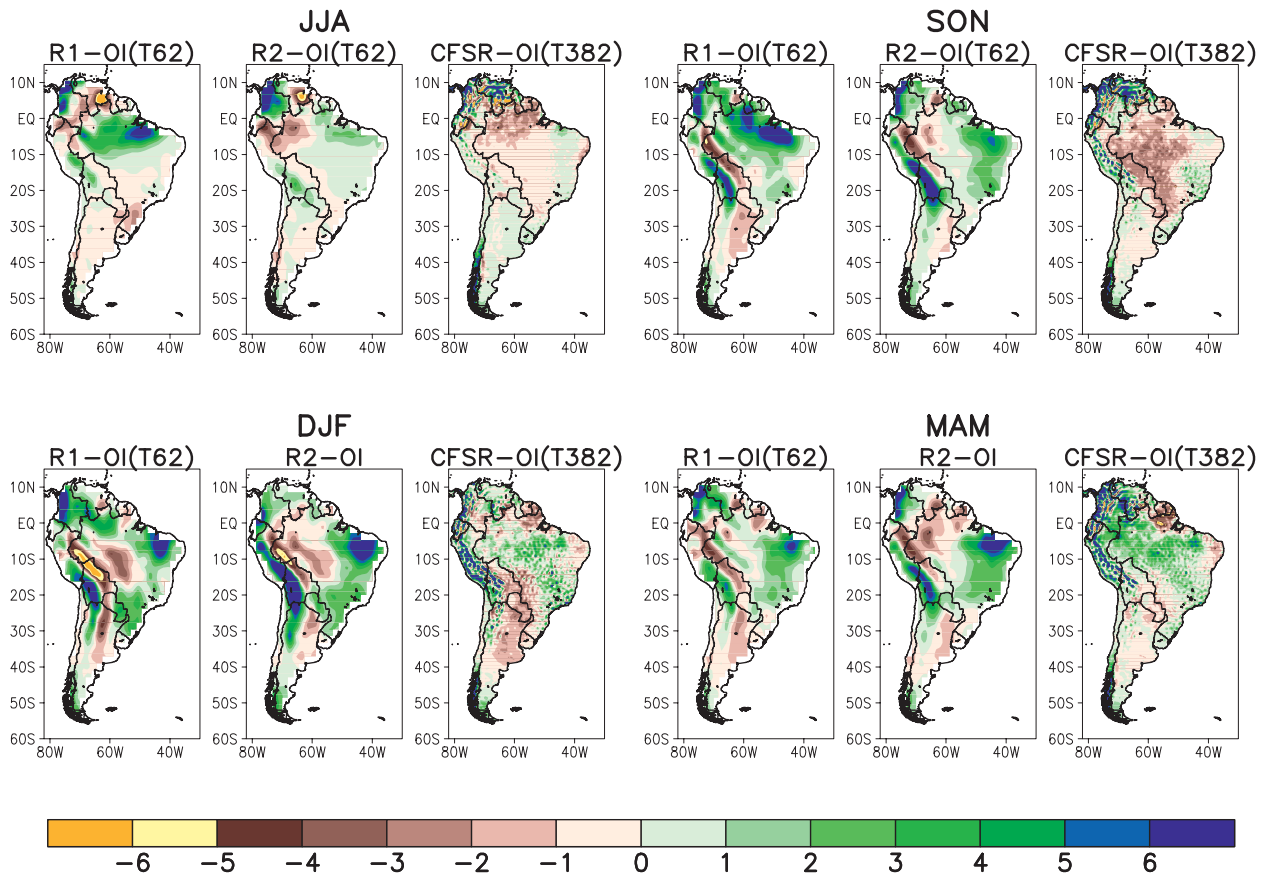


FIG. 3. Mean daily precipitation difference (mm day^{-1}) between R1 and OI(T62), R2 and OI(T62), and CFSR and OI(T382). Results are shown by season and are based on daily data for the period 1979–2006.

Andes (from Peru to Bolivia) and over tropical Brazil near 50°W ; features that are not evident in OI(T62). In DJF the patterns in R1 and R2 are similar to each other, but quite different from OI(T62). OI(T62) shows a maximum in precipitation over west-central Brazil, and relatively light precipitation over northeast Brazil. Both R1 and R2 display a maximum in precipitation near the north coast of northeast Brazil, and a relative minimum in precipitation over west-central Brazil. As in SON, both R1 and R2 display high precipitation amounts over the Andes of Peru and Bolivia, which are not found in OI(T62). In MAM the R1 and R2 patterns are similar to OI(T62), except over the Andes and over western Colombia.

The precipitation patterns over Brazil in CFSR (Fig. 2) show improvements compared to R1 and R2, especially during SON, DJF, and MAM. During DJF the CFSR captures the South Atlantic convergence zone (SACZ) over southeast Brazil. However, as in R1 and R2, CFSR displays a maximum over the Andes (from Ecuador south to northern Argentina), which is not evident in OI(T382). Observations from a rather dense network of stations in

the central Andes (15° – 25°S) during DJFM (Vuille and Keimig 2004) indicate mean daily rainfall rates of 5–8 mm or less, which is consistent with the OI(T382) and OI(T62) gridded analyses in that region. Since the R1, R2, and CFSR indicate mean daily rainfall rates greater than 10 mm, it appears that the reanalyses substantially overestimate rainfall in that region.

The mean daily precipitation differences between the reanalyses (R1, R2, and CFSR) and their corresponding OI analyses are shown in Fig. 3. The CFSR biases are less than those in R1 and R2 in the vicinity of the Andes, probably due to the increase in CFSR resolution (all seasons). The CFSR biases are also less than R1 and R2 over portions of northeastern Brazil (SON, DJF, and MAM). The CFSR dry bias over west-central Brazil (SON) is more extensive than in either R1 or R2. Over the Amazon Basin the CFSR is too dry during the dry season (JJA) and onset phase (SON) of the South American monsoon system (SAMS), and too wet during the peak (DJF) and decay (MAM) phases of the SAMS. CFSR is too dry over Paraguay and the northern two-thirds of Argentina during DJF and too wet over most of southeast Brazil in all seasons.

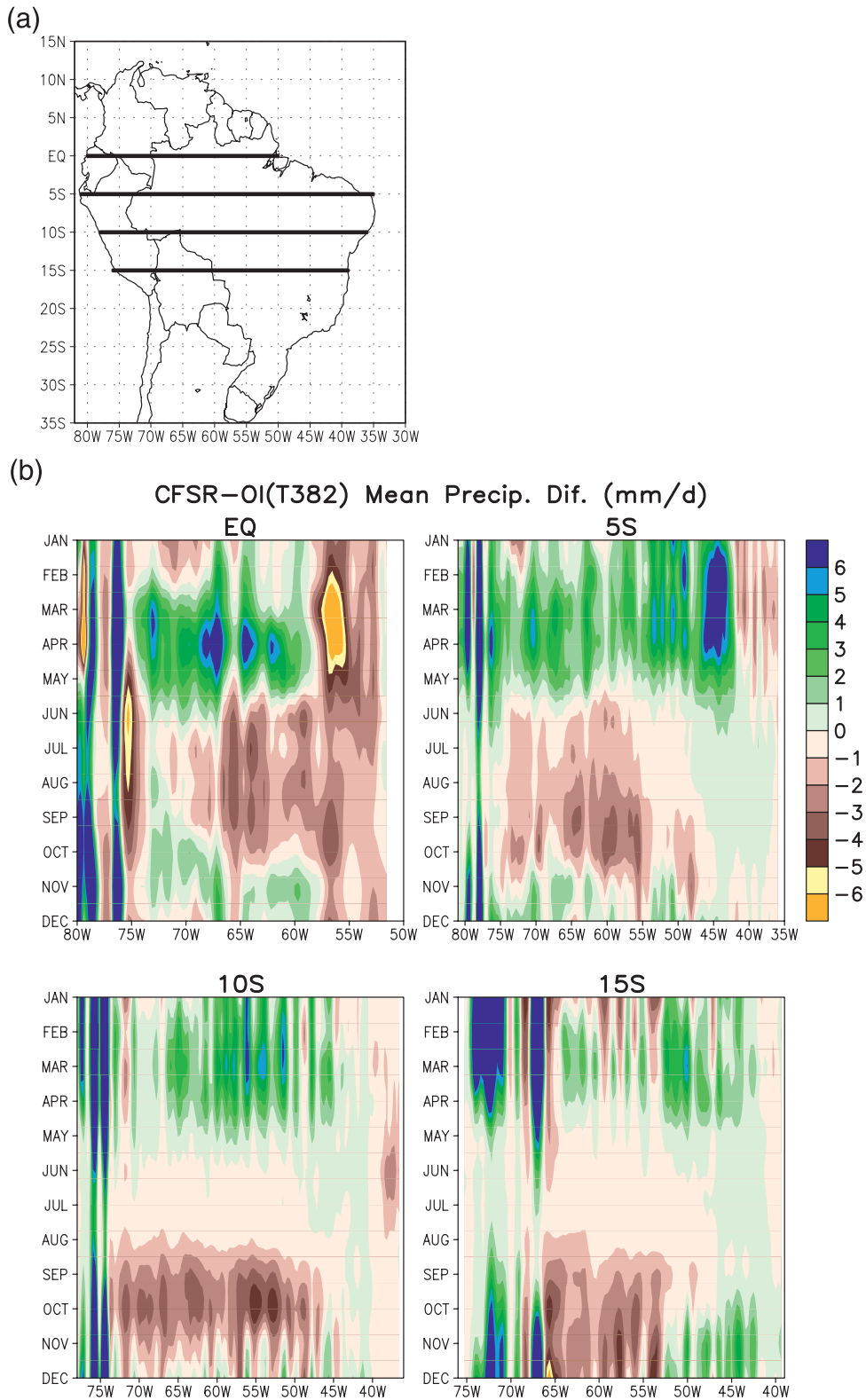


FIG. 4. (a) Representation of the time–longitude sections along the equator, 5°, 10°, and 15°S and (b) time–longitude sections of the mean precipitation difference between the CFSR and OI(T382). Results are based on daily data for the period 1979–2006.

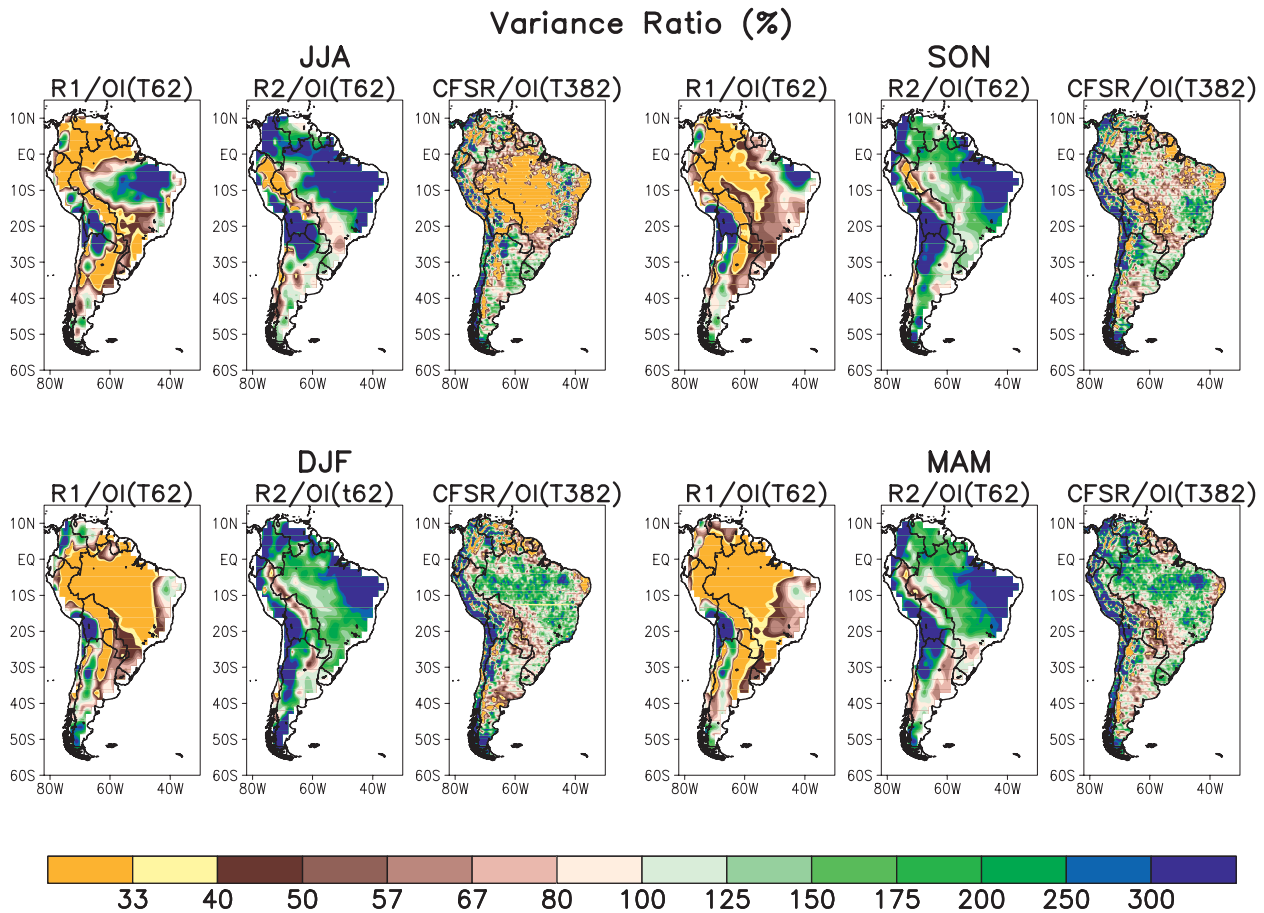


FIG. 5. Variance ratios between R1 and OI(T62), R2 and OI(T62), and CFSR and OI(T382). Results are shown by season and are based on daily data for the period 1979–2006.

Time–longitude sections of the mean precipitation difference between the CFSR and OI(T382) were selected (0° , 5° , 10° , and 15° S) (Fig. 4a) to better depict the biases through the annual cycle (Fig. 4b). At the equator the CFSR is too dry along the Atlantic coast (52° – 57° W) throughout the year. In the central and western Amazon Basin (58° – 74° W) the CFSR is too wet during March–May and too dry during June–October. At 5° S, in the central and western Amazon Basin (55° – 75° W) the CFSR is too wet during February–May and too dry during June–October. At 10° S, in central and western Brazil (45° – 75° W) the CFSR is too wet during January–May and too dry during August–November. At 15° S, in central-western Brazil and eastern Bolivia (50° – 65° W) the CFSR is too wet during February–April and too dry during August–December. In eastern Brazil the CFSR is too wet during October–May. The CFSR is too wet over the Andes throughout the year in all of the cross sections. Possible mechanisms for some of these biases will be discussed in section 4.

The variance ratios and temporal correlations between R1 and OI(T62), R2 and OI(T62), and CFSR and OI(T382) are shown in Figs. 5 and 6, respectively. The temporal correlations were computed using all of the daily precipitation amounts for each month during the entire study period (1979–2006). The variance of the daily precipitation amounts was then used to compute the variance ratios between the reanalyses and observations. The R1 has less variance than observations over most of South America in all seasons. In contrast, R2 has more variance than observations over most of South America in all seasons. The magnitude of the variance bias in CFSR is generally less than in either R1 or R2. The CFSR variance is greater than observed in most areas during DJF and MAM (Fig. 5). The temporal correlations between the three daily reanalyses and the observed precipitation (Fig. 6) are highest over midlatitudes and along the east coast of South America for all seasons. In those regions, synoptic disturbances (e.g., frontal systems and upper-level waves) tend to organize convection.

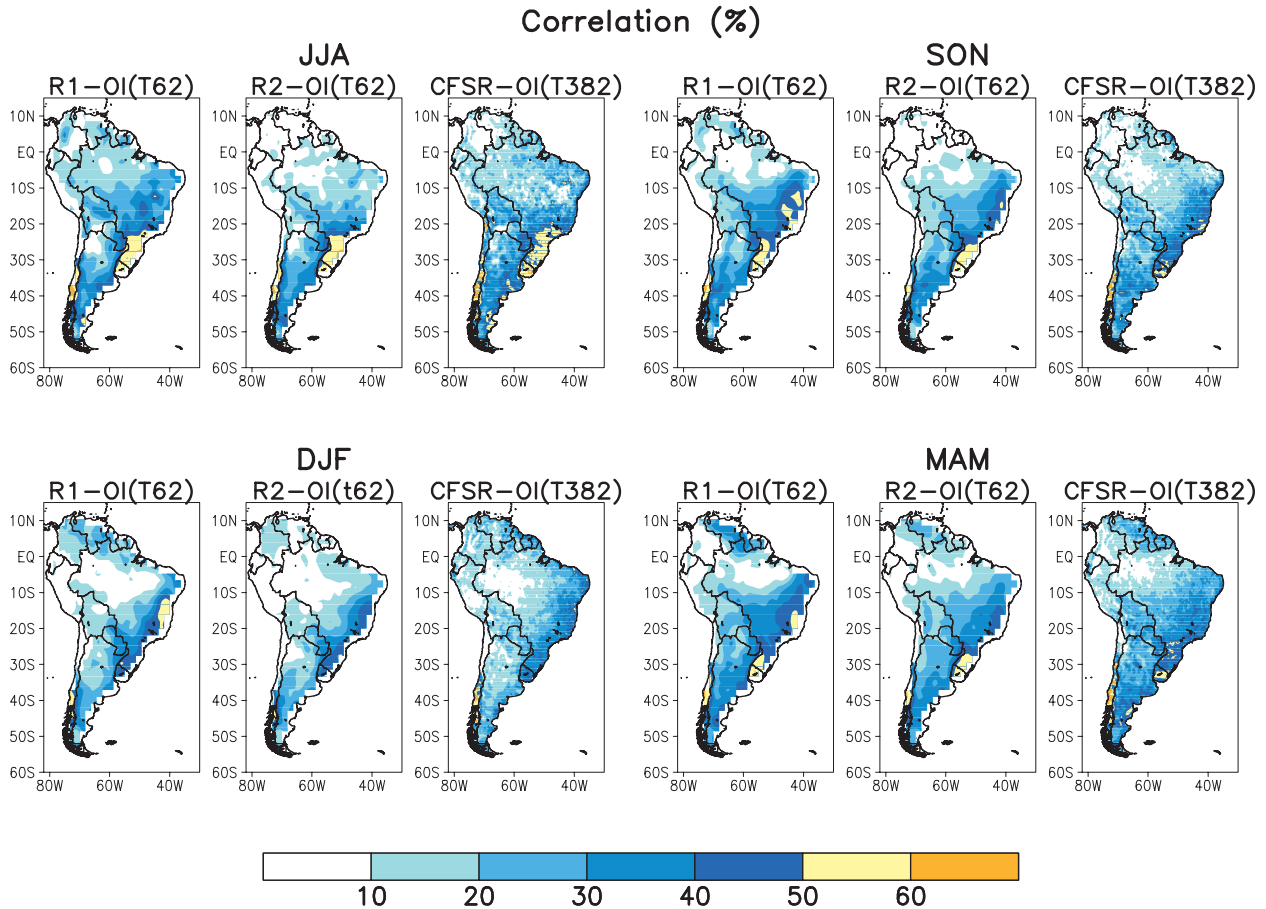


FIG. 6. Temporal correlation between R1 and OI(T62), R2 and OI(T62), and CFSR and OI(T382). Results are shown by season and are based on daily data for the period 1979–2006.

Over tropical latitudes, where convection tends to be less spatially organized on the large scale, correlations are very low for all reanalyses.

b. Probability ratios

The ratio [CFSR/OI(T382)] of mean daily precipitation (Fig. 7) shows that over the Amazon Basin the CFSR is too dry (percent ratio less than 100) during JJA and SON (the dry season and onset phase of the SAMS wet season), and too wet (percent ratio greater than 100) during DJF and MAM (the peak and decay phases of the SAMS wet season). CFSR is too dry over Paraguay and the northern two-thirds of Argentina during DJF and too wet over most of southeast Brazil in all seasons. CFSR is too dry along the east coast of Northeast Brazil during all seasons.

The frequency of occurrence (probability) of daily precipitation exceeding selected thresholds ($P \geq 0.25$ mm, $P \geq 5$ mm, $P \geq 15$ mm, $P \geq 25$ mm) for each month during the entire record (1979–2009) was used to compute

seasonal probability ratios between the CFSR and OI(T382) (Figs. 8a,b). During JJA and SON (Fig. 8a), the CFSR probabilities are too low over the Amazon Basin extending into the SAMS core region (central Brazil) for all thresholds. The bias increases as the threshold amount increases, indicating that the CFSR is not capturing frequency and intensity of precipitation amounts greater than or equal to 5 mm over this region. In contrast, during DJF and MAM (Fig. 8b), the CFSR probabilities are too high for most of northern South America for the threshold $P \geq 0.25$ mm and $P \geq 5$ mm. For these seasons, in particular, the CFSR has too many wet days ($P \geq 0.25$ mm) with low rainfall amounts. CFSR probabilities are too high over southeastern Brazil for all seasons and all thresholds (Figs. 8a,b).

c. Regional biases

To verify in more detail the mean annual cycle of biases between the CFSR and OI(T382), we calculated time series of the mean daily precipitation (not shown)

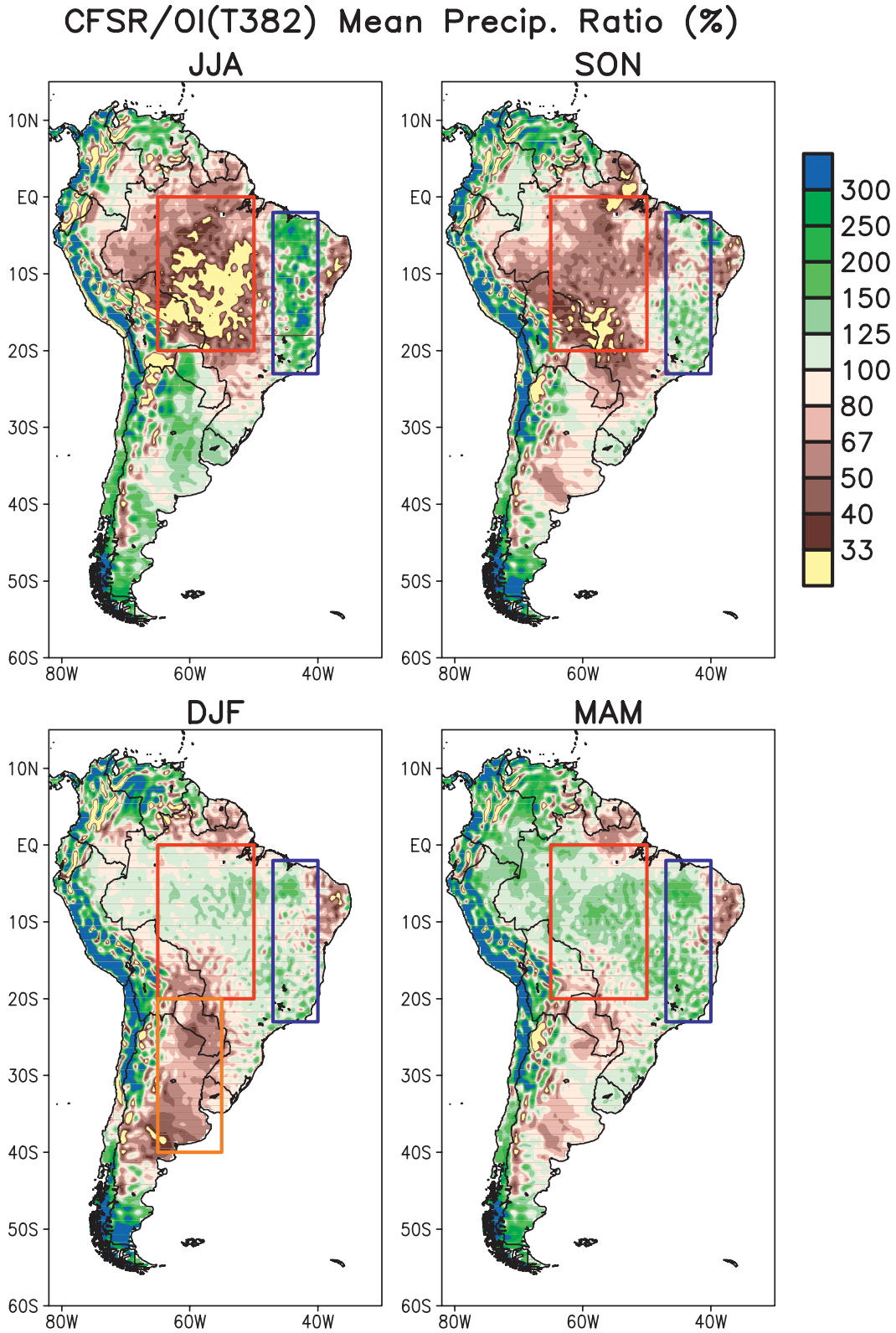


FIG. 7. Percent ratio of mean daily precipitation between CFSR and OI(T382). Results are shown by season and are based on daily data for the period 1979–2006.

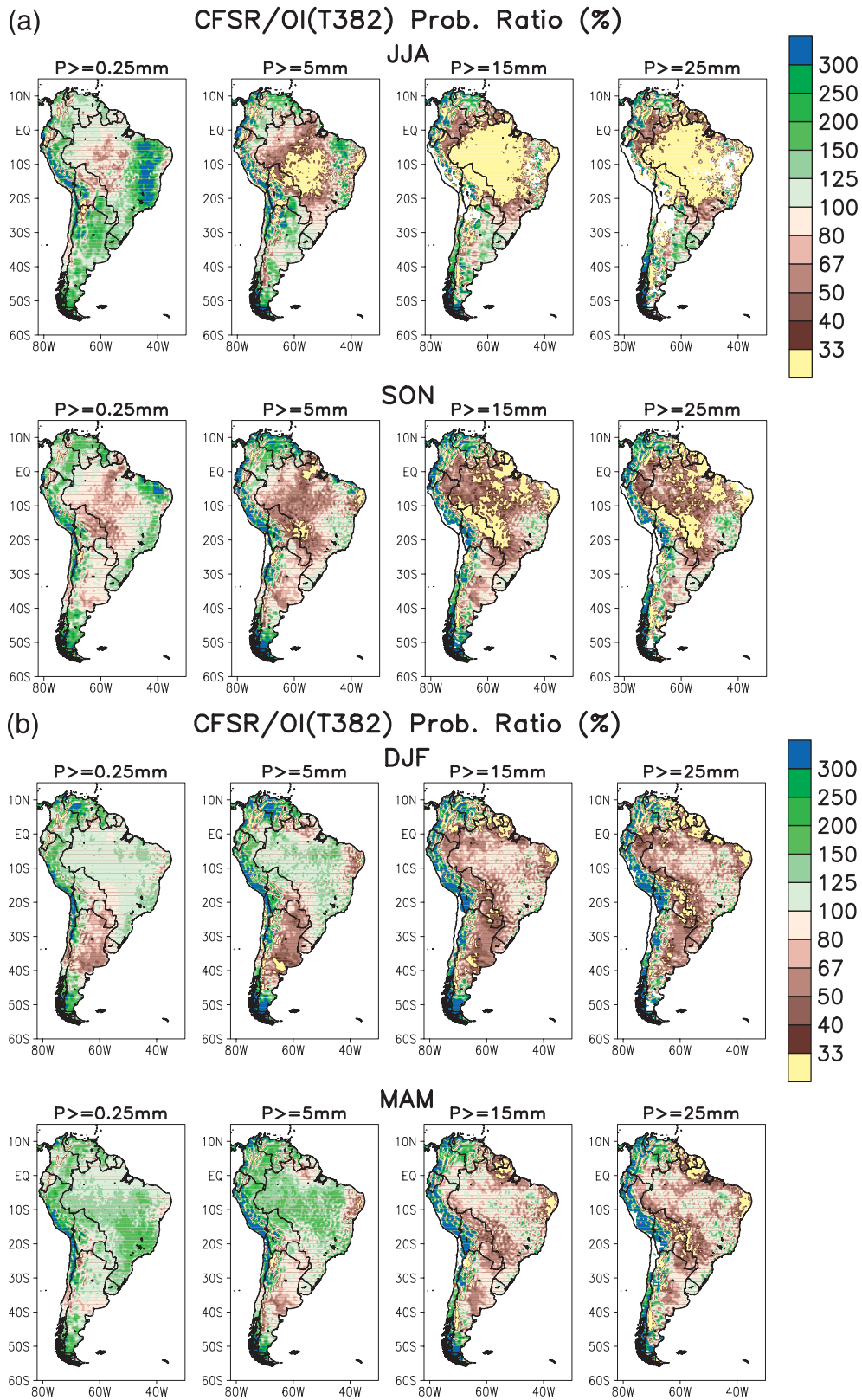


FIG. 8. Percent probability ratio of mean daily precipitation (1979–2006) between CFSR and OI(T382) for (a) JJA and SON and (b) DJF and MAM.

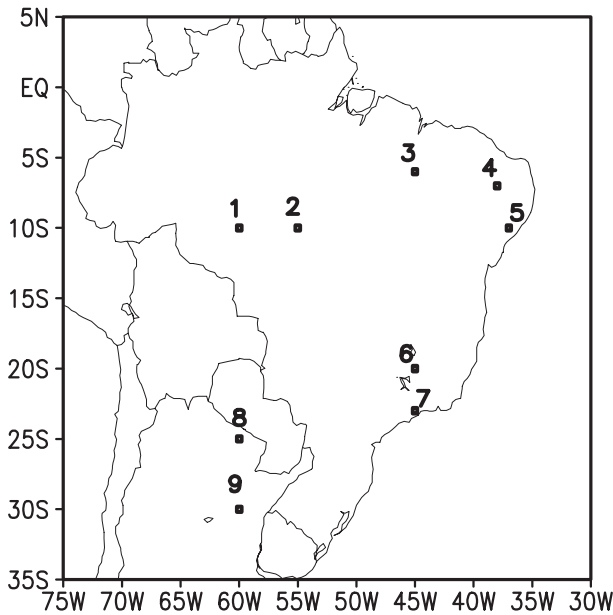


FIG. 9. Reference grid points for the Amazon Basin, northeast Brazil, southeast Brazil, and central South America.

and probabilities for selected thresholds at grid points (Fig. 9) over the Amazon Basin, northeast Brazil, southeast Brazil, and central South America.

For the two grid points over the Amazon Basin, 10°S – 60°W (1) and 10°S – 55°W (2), the CFSR is too dry during July–October (onset phase of the SAMS), and too wet during January–May (peak and decay phases of the SAMS; Fig. 4b, time–longitude section for 10°S). For these grid points the CFSR probabilities (Fig. 10) generally exceed the observed probabilities during January–May for the three lightest thresholds (0.25, 5, and 10 mm), while there is good agreement between CFSR and OI(T382) for the three highest thresholds (15, 20, and 25 mm). The CFSR probabilities are generally less than observed for all thresholds during the period July–December.

Over northeast Brazil the CFSR is drier than OI(T382) throughout the annual cycle for the two grid points along the coast, 7°S – 38°W (4) and 10°S – 37°W (5) (Fig. 4b, time–longitude section for 10°S). For the grid point, 7°S – 38°W (4), the CFSR probabilities (Fig. 11) are too low during January–March, and slightly too high during June–December for the lightest threshold. For all other thresholds CFSR probabilities are too low during November–June. For the grid point, 10°S – 37°W (5), the CFSR probabilities are similar to OI(T382) throughout the annual cycle for the lightest threshold ($P \geq 0.25$ mm). For higher thresholds the CFSR probabilities are too low, especially during April–July.

For the grid point, 6°S – 45°W (3) (Fig. 4b, time–longitude section for 5°S), CFSR is wetter than OI(T382) from December to July and similar to OI(T382) during the other months. The CFSR probabilities for this grid point (Fig. 11) exceed the observed probabilities throughout the annual cycle for the lightest thresholds (0.25 mm). For $P \geq 5$ and $P \geq 10$ mm, probabilities are higher in the CFSR from January to July and close to observed during August–December. For thresholds larger than 15 mm CFSR probabilities are very similar to OI(T382), except slightly lower during September–December.

Over southeast Brazil the CFSR is wetter than OI(T382) throughout the year near Sao Paulo [23°S – 45°W (7)] and in the vicinity of the coastal mountains [20°S – 45°W (6); see Fig. 3]. The CFSR probabilities (Fig. 12) generally exceed the observed probabilities throughout the year for the two lightest amounts (0.25 and 5 mm). There is good agreement between CFSR and OI(T382) at 20°S – 45°W (6) for the four highest amounts. However, for the grid point near the coast, 23°S – 45°W (7), the CFSR probabilities exceed OI(T382) during the wet season (November–April) for all thresholds.

Over central South America the CFSR is too dry during December–March (wet season) and slightly too wet during May–August (dry season) for both selected stations: 25°S – 60°W (8) and 30°S – 60°W (9); see Fig. 3]. For both stations, the CFSR probabilities (Fig. 13) are less than observed probabilities for all thresholds during December–March (wet season), and slightly exceed observed probabilities during June–August (dry season) for the three lightest thresholds (Fig. 13).

Table 1 shows the seasonal pattern correlations of mean (1979–2006) daily precipitation between observations and the three reanalyses over the region 0° – 35°S , 35° – 65°W (i.e., most of Brazil–SAMS core region). CFSR shows considerably higher pattern correlations compared to R1 and R2, especially during the wet seasons (SON, DJF, and MAM). The somewhat lower pattern correlation between the CFSR and OI(T382) in SON is undoubtedly related to the dry bias in CFSR during the onset of the SAMS wet season.

4. Discussion and conclusions

There is an obvious need for improved understanding and prediction of intraseasonal-to-interannual variability of precipitation, as an important component of an overall strategy to mitigate the societal impacts of extreme events, such as droughts and floods. To address this need the NCEP has developed a new generation of reanalysis products as part of the Climate Forecast System Reanalysis and Reforecast (CFSRR; Saha et al. 2006) project. This project provides an improved climate

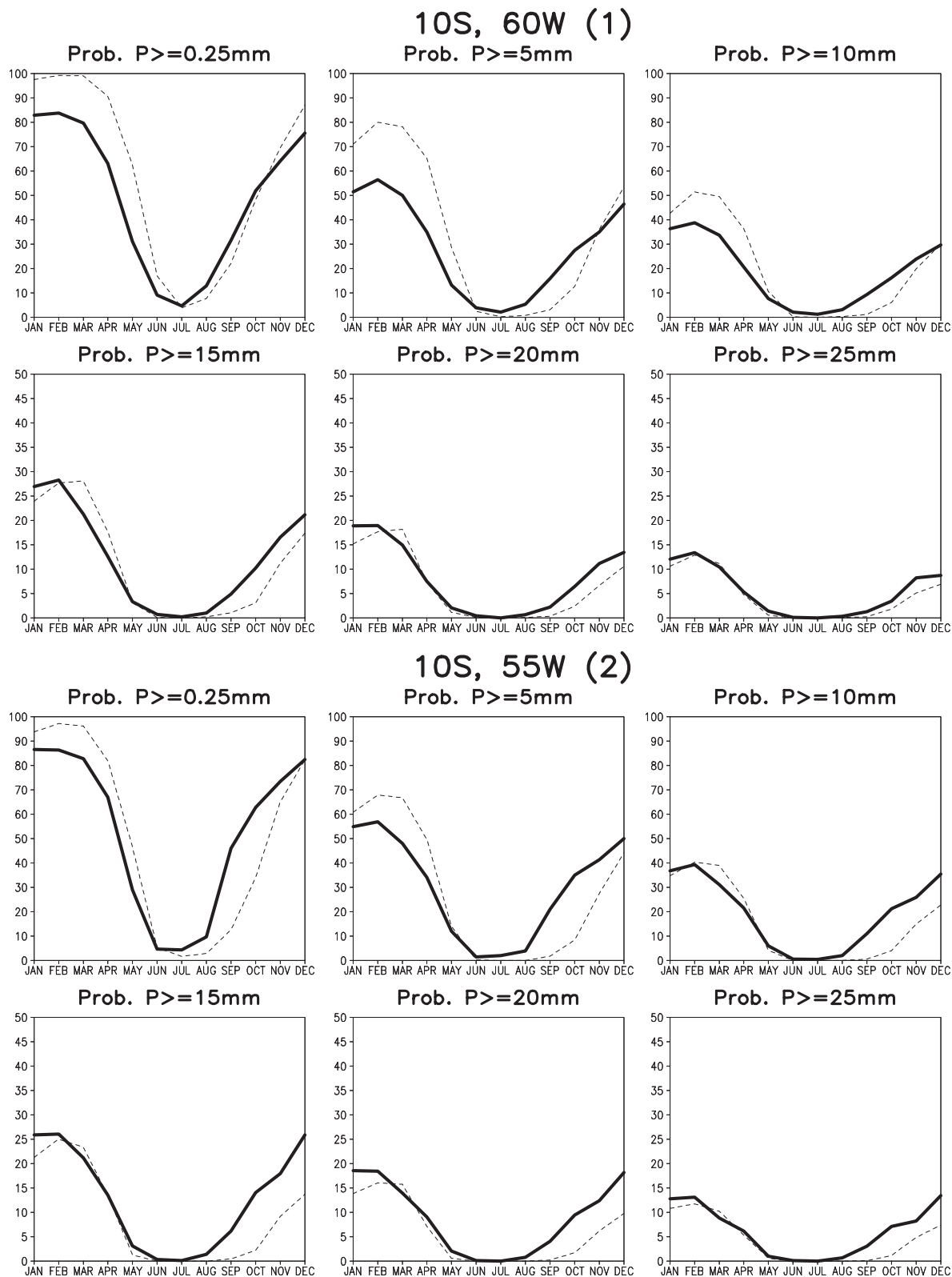


FIG. 10. Annual cycle of the probability (%) exceeding selected threshold ($P \geq 0.25$ mm, $P \geq 5$ mm, $P \geq 15$ mm, $P \geq 25$ mm) for the grid points 10°S–60°W (1) and 10°S–55°W (2) in the Amazon Basin [CFSR (dashed line) and OI(T382) (solid line)]. Results are based on daily data for the period 1979–2006.

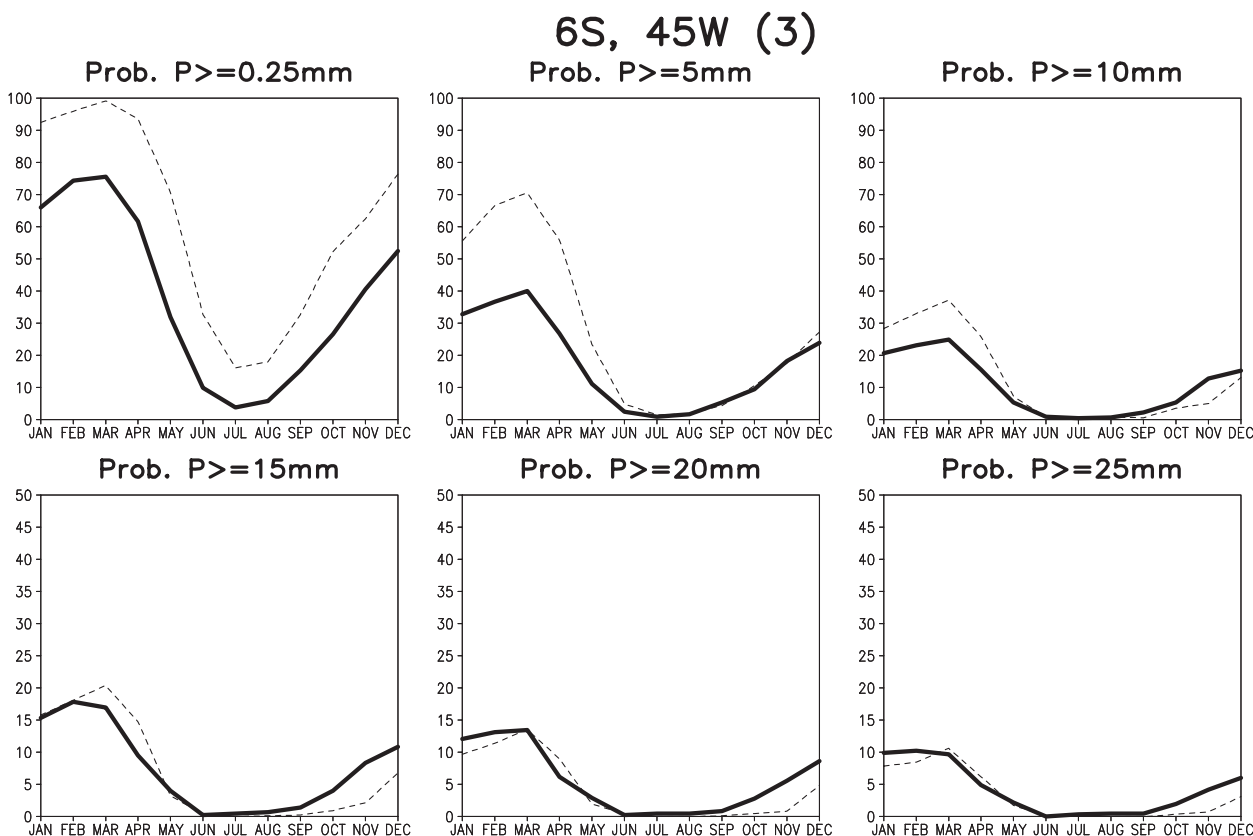


FIG. 11. Annual cycle of the probability (%) exceeding selected threshold ($P \geq 0.25$ mm, $P \geq 5$ mm, $P \geq 15$ mm, $P \geq 25$ mm) for the grid points 6°S – 45°W (3), 7°S – 38°W (4), and 10°S – 37°W (5) in northeast Brazil [CFSR (dashed line) and OI(T382) (solid line)]. Results are based on daily data for the period 1979–2006.

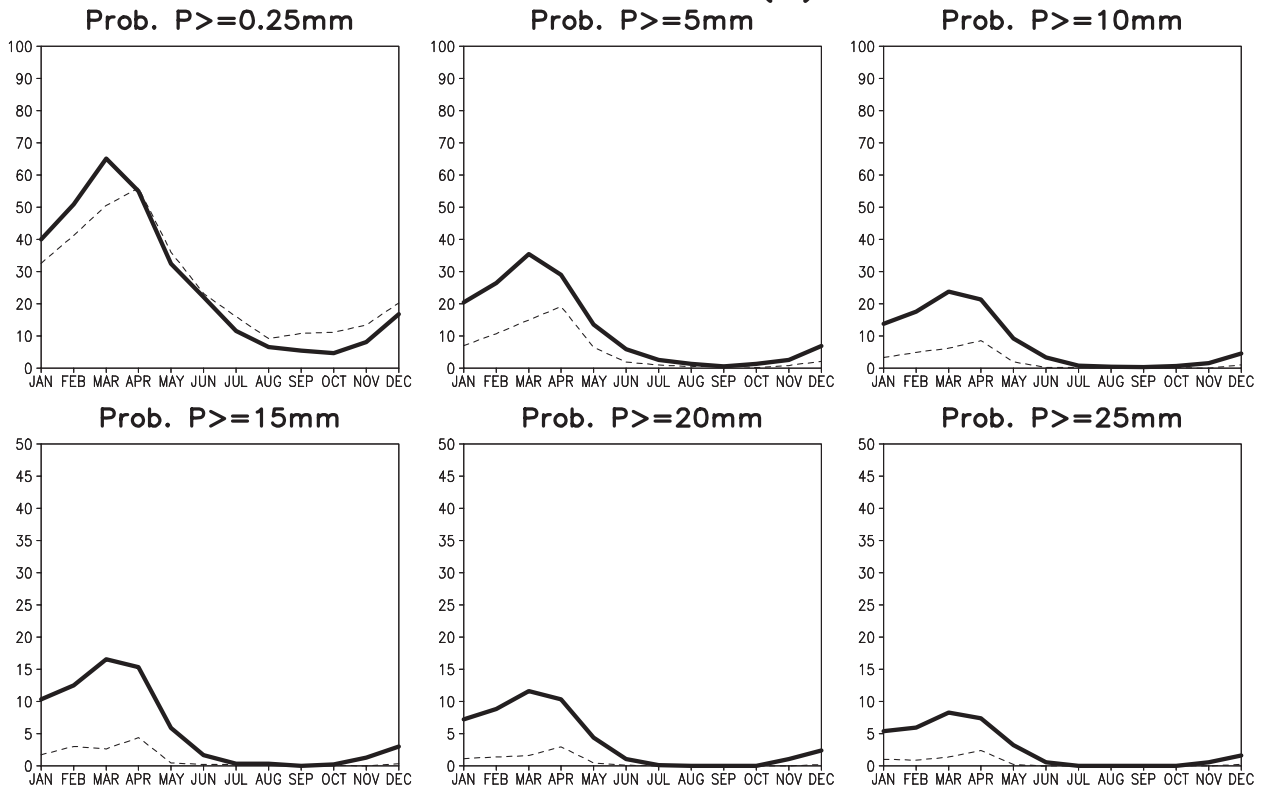
dataset for research and an improved forecast system for intraseasonal and seasonal forecasts, which can be used by a wide range of decision makers in agriculture, water resource management, emergency, and economic planning, etc. Thus, there is a need to evaluate/validate CFSR, in particular to document the extent to which biases in previous reanalysis datasets have been addressed.

In this study, we compared the CFSR model-based precipitation over South America with observations. The CFSR shows notable improvements in the large-scale precipitation patterns compared with the previous reanalyses (R1 and R2). These improvements are reflected in the mean midtropospheric (500 hPa) vertical motion (ω) patterns, especially during December–February (Fig. 14). The CFSR displays a minimum in ω (maximum rising motion) near 10°S , 60°W in the southern Amazon Basin, which is near the maximum in precipitation displayed in the OI analyses (DJF patterns in Figs. 1 and 2). In contrast, both R1 and R2 display minima in ω outside of the region of observed maximum

precipitation. The pattern correlations between the 500-hPa vertical motion (ω) and observed precipitation fields (regridged to 2.5° latitude–longitude to match the resolution of the reanalysis ω fields) for R1, R2, and CFSR in DJF over the SAMS core region (0° – 35°S , 35° – 65°W) are (i) -0.72 for R1, (ii) -0.60 for R2, and (iii) -0.87 for CFSR. The DJF CFSR 500-hPa ω pattern agrees much better with the observed mean daily precipitation pattern than do R1 and R2.

In spite of these improvements in the CFSR patterns of precipitation, substantial biases in intensity and frequency of occurrence of rainfall events exist in the CFSR. The dry bias in the CFSR during the onset phase of the SAMS wet season and wet bias during the peak and decay phases of the SAMS wet season may be related to model biases in soil moisture and/or evapotranspiration, and the effects that those have on initiating precipitation in the model. During December–May, when soil moisture and evapotranspiration are high, the CFSR is too wet. During July–October, when soil

7S, 38W (4)



10S, 37W (5)

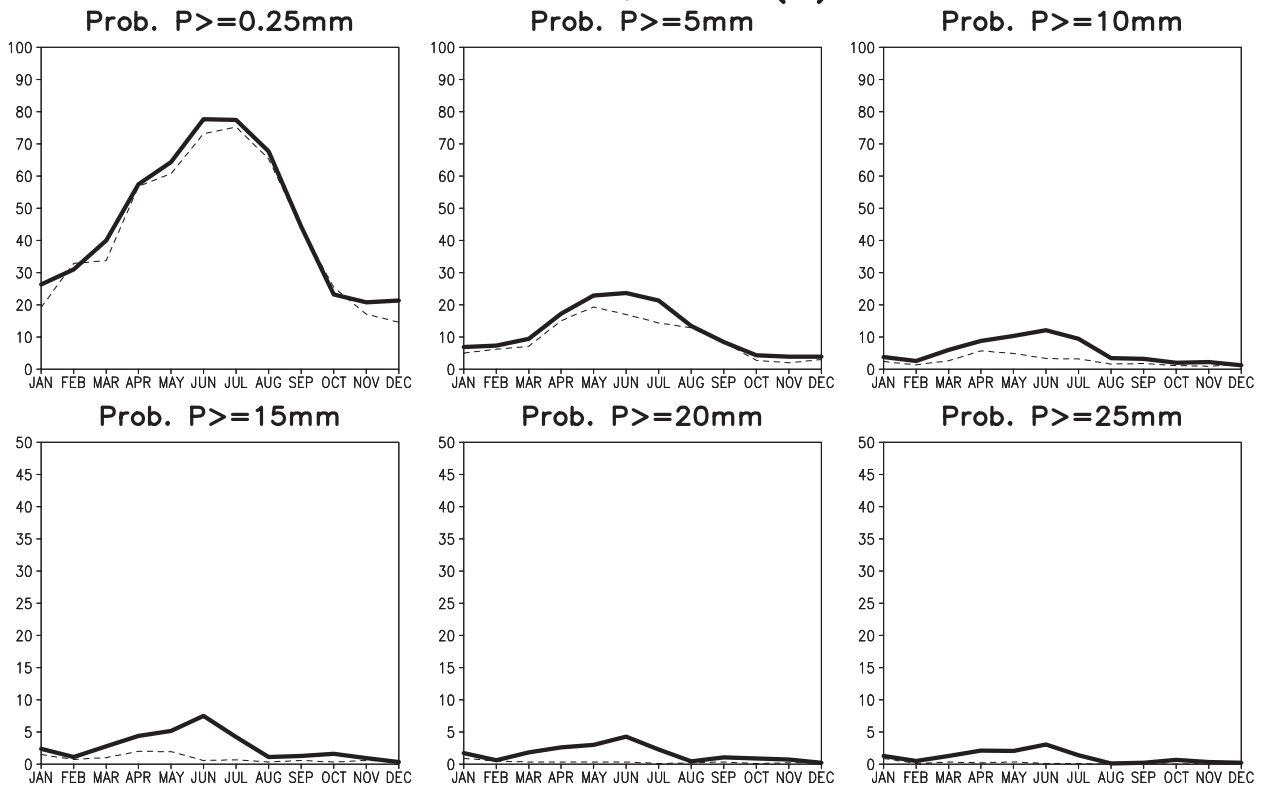
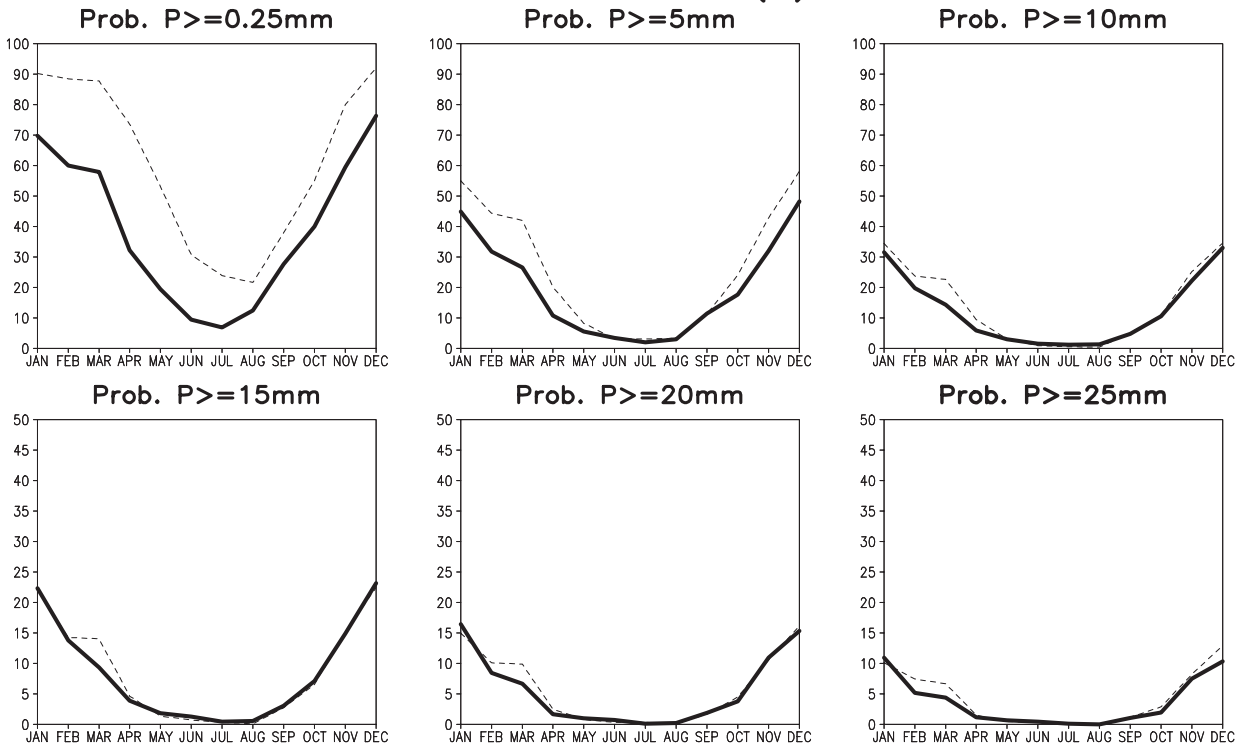


FIG. 11. (Continued)

20S, 45W (6)



23S, 45W (7)

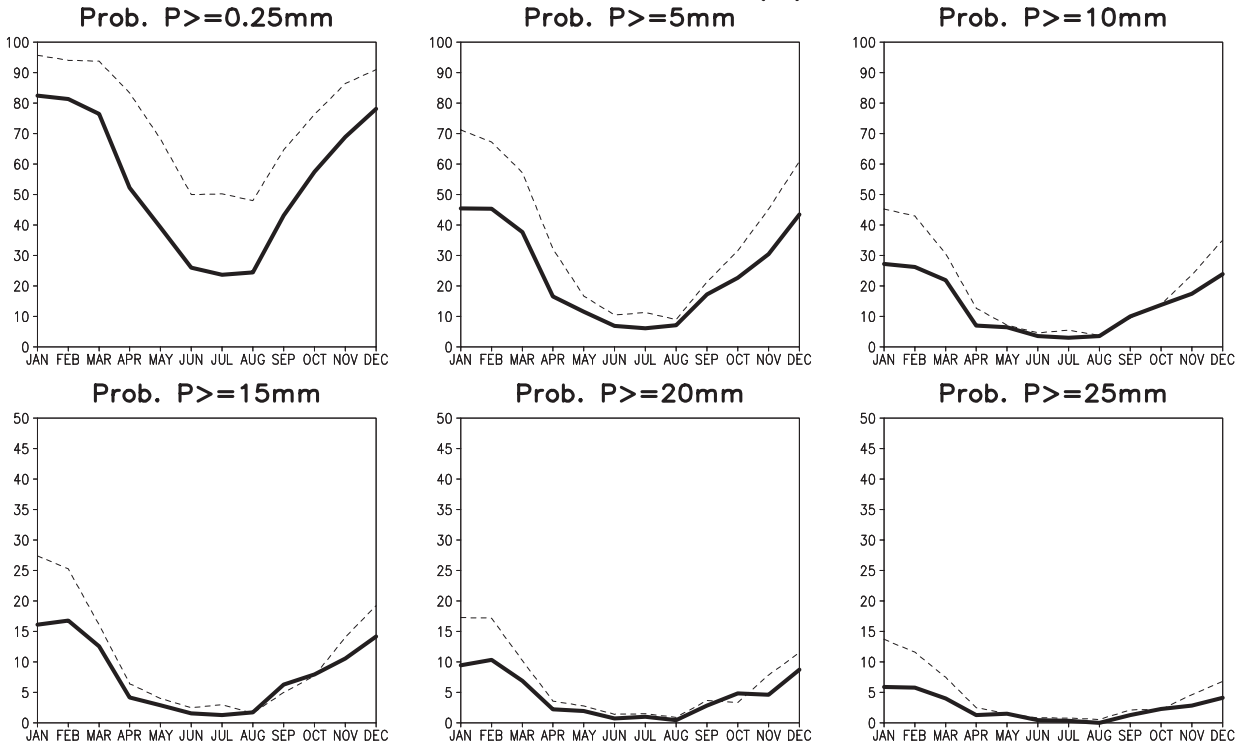


FIG. 12. Annual cycle of the probability (%) exceeding selected threshold ($P \geq 0.25\text{ mm}$, $P \geq 5\text{ mm}$, $P \geq 15\text{ mm}$, $P \geq 25\text{ mm}$) for the grid points 20°S–45°W (6) and 23°S–45°W (7) in southeast Brazil [CFSR (dashed line) and OI(T382) (solid line)]. Results are based on daily data for the period 1979–2006.

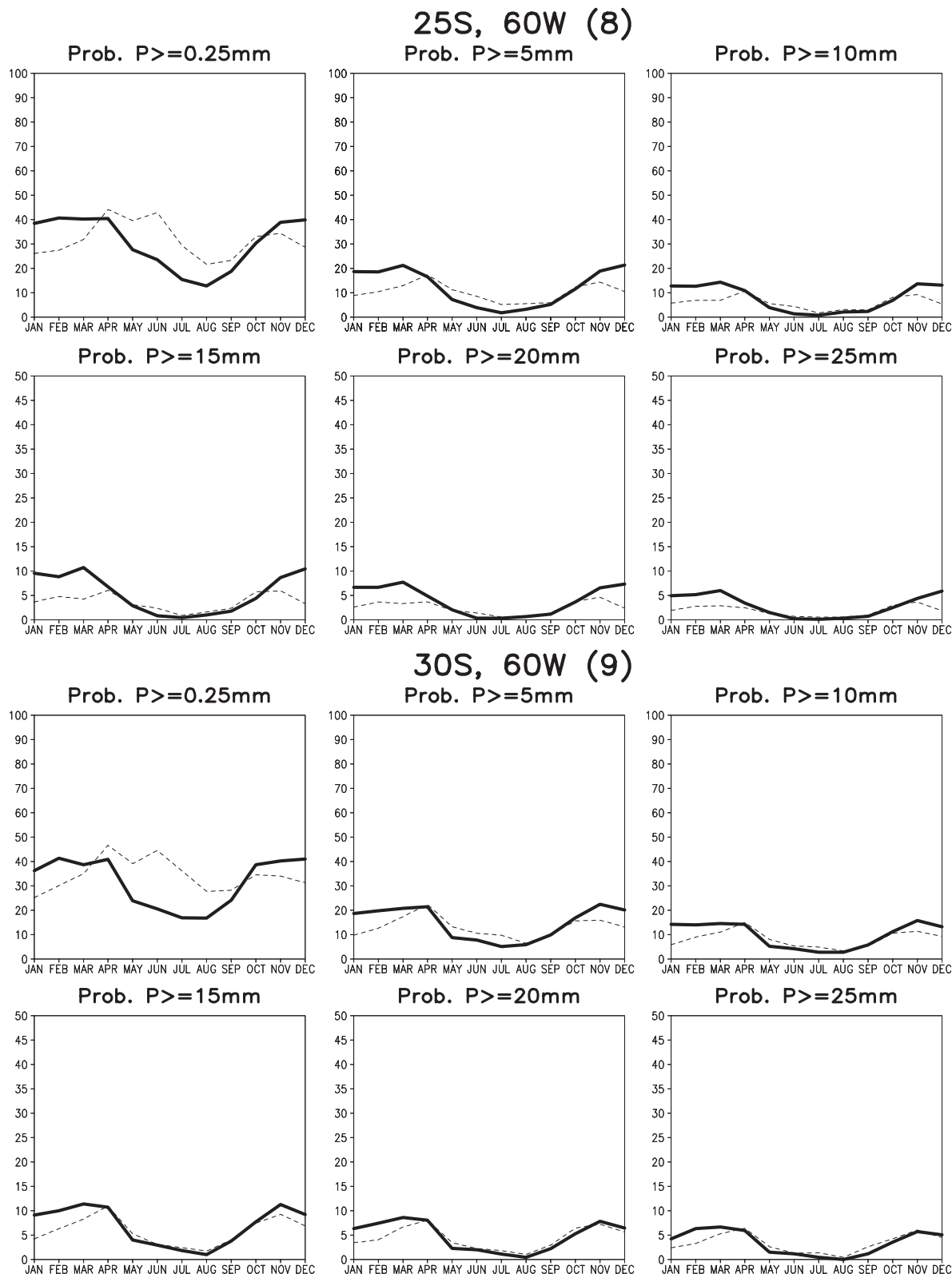


FIG. 13. Annual cycle of the probability (%) exceeding selected threshold ($P \geq 0.25$ mm, $P \geq 5$ mm, $P \geq 15$ mm, $P \geq 25$ mm) for the grid point 25°S–60°W (8) and 30°S–60°W (9) in central South America [CFSR (dashed line) and OI(T382) (solid line)]. Results are based on daily data for the period 1979–2006.

TABLE 1. Pattern correlations for the SAMS core region (0° – 35° S, 35° – 65° W).

Season	R1 vs OI(T62)	R2 vs OI(T62)	CFSR vs OI(T382)
DJF	0.46	0.47	0.85
MAM	0.80	0.67	0.86
JJA	0.72	0.88	0.86
SON	0.43	0.30	0.61

moisture and evapotranspiration are low, the CFSR is too dry.

In addition, there is a dry bias in the CFSR in coastal areas near the mouth of the Amazon (the equator section in Fig. 4b) and along the east coast of Northeast Brazil (sections along 5° and 10° S, Fig. 4b), which may indicate that the CFSR is not capturing the intensity and/or frequency of land–sea-breeze induced rainfall that is observed in this region (Kousky 1980; Janowiak et al. 2005). Furthermore, the higher-than-observed probabilities of light rainfall events and less-than-observed probabilities of heavy rainfall events in the CFSR for many areas in Brazil during DJF and MAM (Fig. 8) suggest that the CFS may be too quick to initiate diurnal convective rainfall, resulting in weaker events. These hypotheses need to be explored in a detailed evaluation of the model diurnal cycle of precipitation and related variables.

Rainfall amounts in all of the reanalyses (R1, R2, and CFSR) are too high over the mountains. However, there are definite improvements in the CFSR precipitation pattern near the Andes, probably resulting from the increased spatial resolution in CFSR.

In this study a straight comparison was made between the CFSR and OI(T382), and between R1/R2 and OI(T62), to document the biases and demonstrate improvements in the precipitation analyses. Some of our results suggest possible causes for the biases that could be explored by means of a series of model experiments made at the same model resolution, but with changes in the model physical parameterizations. Future studies will further explore the possible causes for the observed biases, in order to provide model developers with additional information that could lead to model improvements.

Acknowledgments. The authors thank Pingping Xie for providing the historical OI(T62) and OI(T382) data sets, Wesley Ebisuzaki and Emily Becker for preparing the global CFSR precipitation dataset, and Wanqiu Wang and Pingping Xie for providing comments and suggestions on an earlier draft of this paper. In addition, the authors thank the three anonymous reviewers for their comments and suggestions, which led to improvements in the paper.

DJF 500–hPa VVEL 1979–2006

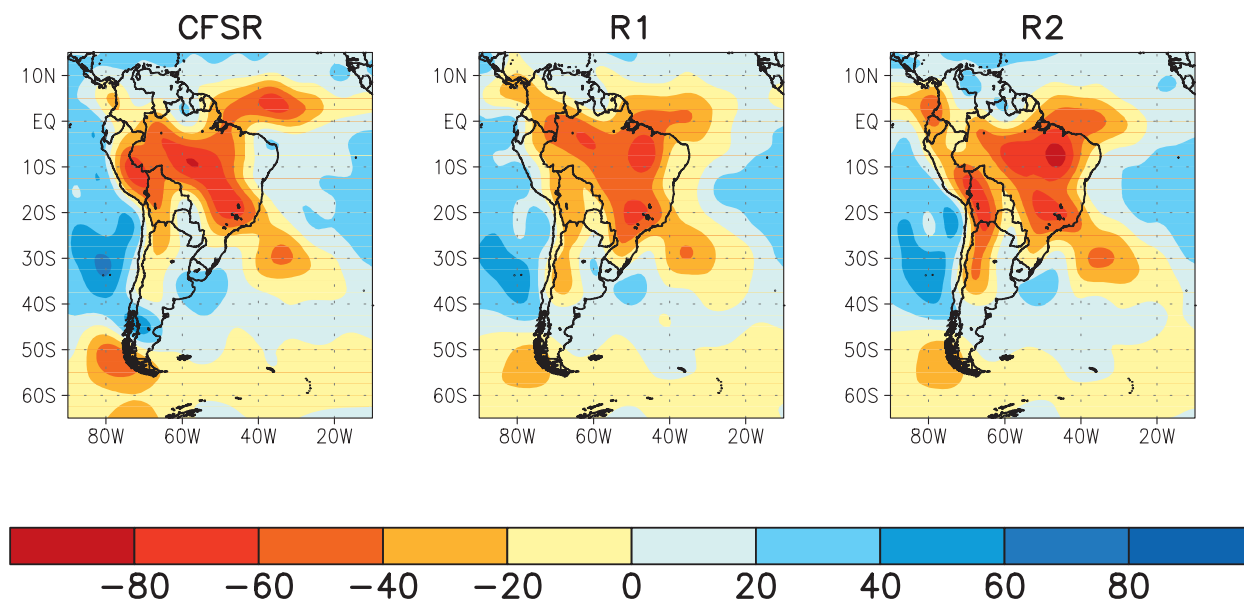


FIG. 14. Mean vertical motion (ω , hPa day^{-1}) during DJF (1979–2006) for CFSR, R1, and R2.

REFERENCES

- Chen, M., W. Shi, P. Xie, V. B. S. Silva, V. E. Kousky, R. Wayne Higgins, and J. E. Janowiak, 2008: Assessing objective techniques for gauge-based analyses of global daily precipitation. *J. Geophys. Res.*, **113**, D04110, doi:10.1029/2007JD009132.
- Gandin, L. S., 1965: *Objective Analysis of Meteorological Fields*. Israel Program for Scientific Translations, 242 pp.
- Higgins, R. W., W. Shi, E. Yarosh, and R. Joyce, 2000: *Improved United States Precipitation Quality Control System and Analysis*. NCEP/Climate Prediction Center Atlas 7, 40 pp. [Available online at http://www.cpc.ncep.noaa.gov/research_papers/ncep_cpc_atlas/7/index.html.]
- Janowiak, J. E., V. E. Kousky, and R. J. Joyce, 2005: Diurnal cycle of precipitation determined from the CMORPH high spatial and temporal resolution global precipitation analyses. *J. Geophys. Res.*, **110**, D23105, doi:10.1029/2005JD006156.
- Kalnay, E., and Coauthors, 1996: The NCEP/NCAR 40-Year Reanalysis Project. *Bull. Amer. Meteor. Soc.*, **77**, 437–471.
- Kanamitsu, M., W. Ebisuzaki, J. Woollen, S.-K. Yang, J. J. Slingo, M. Fiorino, and G. L. Potter, 2002: NCEP–DOE AMIP-II Reanalysis (R-2). *Bull. Amer. Meteor. Soc.*, **83**, 1631–1643.
- Kousky, V. E., 1980: Diurnal rainfall variation in Northeast Brazil. *Mon. Wea. Rev.*, **108**, 488–498.
- Saha, S., and Coauthors, 2006: The NCEP Climate Forecast System. *J. Climate*, **19**, 3483–3517.
- , and Coauthors, 2010: The NCEP Climate Forecast System Reanalysis. *Bull. Amer. Meteor. Soc.*, **91**, 1015–1057.
- Silva, V. B. S., V. E. Kousky, W. Shi, and R. W. Higgins, 2007: An improved gridded historical daily precipitation analysis for Brazil. *J. Hydrometeor.*, **8**, 847–861.
- Vuille, M., and F. Keimig, 2004: Interannual variability of summertime convective cloudiness and precipitation in the central Andes derived from ISCCP-B3 data. *J. Climate*, **17**, 3334–3348.